Journal Name

ARTICLE

Ethylenediamine Mediated Luminescence Enhancement of Pollutant Derivatized Carbon Quantum dots for Intracellular Trinitrotoluene detection: Soot to Shine

S. Devi[a], Raju K Gupta[b], A. K. Paul[c], Vinay Kumar[d], AbhaySachdev[a], P. Gopinath[d] and *S. Tyagi[a]

[a]Analytical Techniques Division, CSIR-CSIO, Chandigarh, India

[b]Indian Institute of Technology, Kanpur, Uttar Pradesh, India

[c]DeshBhagat University, Fatehgarh Sahib, Punjab, India

[d]Indian Institute of Technology Roorkee, Roorkee, Uttarakhand, India

*Corresponding Author Postal Address: Analytical Techniques Division, CSIR-CSIO, Chandigarh 160030, India Tel.: +91-172-2642545 (O); Fax: + 91-172-2657267

E-mail: matsachin@gmail.com, sachintyagi@csio.res.in (Dr. SachinTyagi)

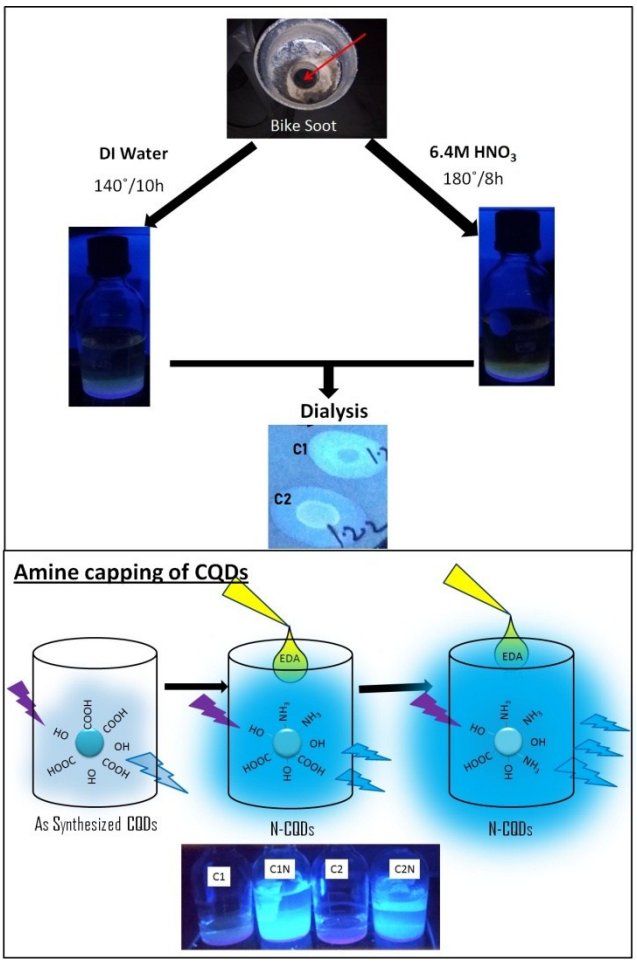

Fig. S1: Schematic illustration for the synthesis of C1 and C2 from bike soot.

Characterizations

Hot air oven (Navyug India Q-5247) was used for hydrothermal synthesis of C1 and C2 in Teflon lined autoclave bottle. The CQD solutions were initially visualized in UV illuminator (Laby Model-T1-50).The absorption and emission properties were studied using UV-visible (Varian) and photoluminescence spectroscopy (PL, Carry Varian) respectively. The vibrational studies were performed by FT-IR (Thermo-Scientific Smart Omni-Transmission Nicolet iS10 spectrometer) and Raman (inViaRaman Renishaw) spectrophotometers. The size and morphology of CQDs were measured by using transmission electron microscope (model TEM: JEOL-JEM 2100).X-Ray Diffraction patterns were obtained by Xpert-Pro-X (Cu-Kα radiation).DLS Zetasizer (ZS90 series) was used for hydrodynamic size and surface charge studies of the CQDs.

Results & Discussion

The XRD spectra were explored for the structural analysis of the as-synthesized C1 and C2 (Fig. S2a, b). The amorphous nature of these QDs is confirmed from the broad diffraction peaks of C1 and C2at 2theta 22.5˚ and 22.8˚ respectively. This can be credited to the closely packed carbon atoms having surface functionalities in QDs.[1]

The surface functionalities of C1 and C2 were studied using Raman spectroscopy and spectra are shown in figure S2c. The sharp D and G peaks of C1 are observed at ~1344 and 1537cm^{-1}while D and G peak of C2 are present at ~1344 and 1506 cm^{-1}. It clearly confirms the synthesis of CQDs from bike soot sue to the hybridization state of carbon. These D-band represents the defect mode and G-band correspond to E2g mode, which point the sp^2 graphitic defect sites in amorphous carbon. The ratio of D and G bands intensities (ID/IG) was calculated for both the C1 and C2. The ID/IG for C1 and C2 are observed to be ca. 1.21 and 0.925 respectively. It might be attributed to the presence of structural defects in these CQDs leading in out of plane vibrations.[2] In addition, these XRD and Raman results are found in complete accordance to their SAED data.

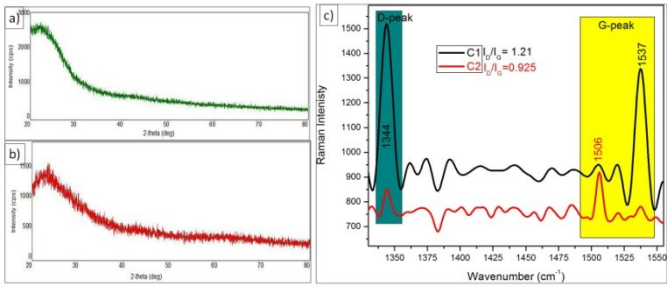

Fig. S2: (a) and (b) XRD spectra of C1 and C2 respectively; (c) Raman spectra of C1 and C2.

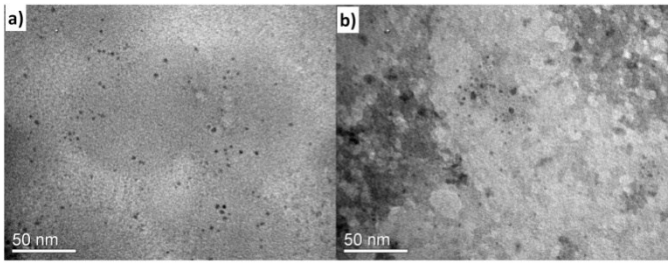

Fig. S3: Showing the TEM micrograph of (a) C1N and (b) C2N.

The hydrodynamic size and surface potentials of C1 and C2 before and after amine functionalization were measured by DLS. The hydrodynamic sizes of these QDs are shown in figure S4.The average hydrodynamic diameter of C1 and C2 are 5.4d.nm and 7.45d.nm respectively. The presence of two peaks in the DLS spectra of C2 depicts the less uniformity in their size in comparison to the C1 while both the samples C1 and C2 represent appreciative dispersibility in aqueous solution. It can be attributed to

electrostatic repulsion between the charged QDs resulting in their electro stearic stabilization.[3] This DLS data is found to be in complete agreement with the TEM results. The average hydrodynamic size of C1N and C2N is found as 8.9d.nm and 21.11d.nm respectively. So, after the treatment of QDs with EDA, the clear increase in their hydrodynamic size can be noticed (Fig S4c, d), which confirms the amine functionalization on the QD surfaces.

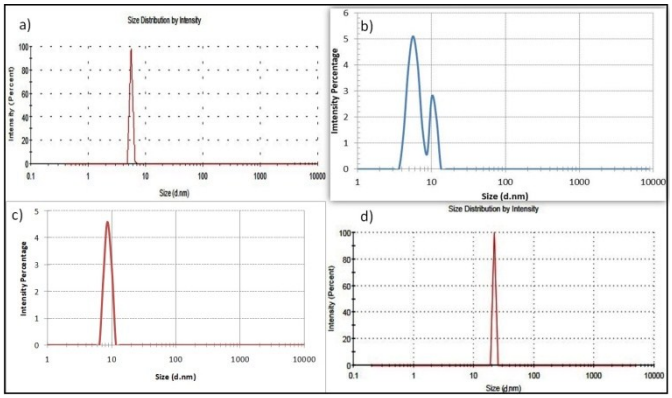

Fig. S4:Showing the hydrodynamic size of (a) C1; (b) C2; (c) C1N; and (d) C2N.

Zeta potential of these QDs (Fig. S5) was also measured. It was perceived that C1 has -17.1mV (pH 6) surface charge (Fig. S5a), which can be due to the presence of the carboxyl groups on the surface. While the less but positive charge on C2 surface (Fig. S5b) may be explained via the method of their synthesis in the presence of nitric acid leading in any possible interaction of nitrogen group on C2 surface functionalities. After amine functionalization, the surface charge of +60.2mV and +64.7mV was observed on C1N and C2N respectively (Fig. S5c, d). It can be attributed to the presence of positively charged amine groups and their interaction with carboxylic groups on their surfaces resulting in increase in net positive charge.

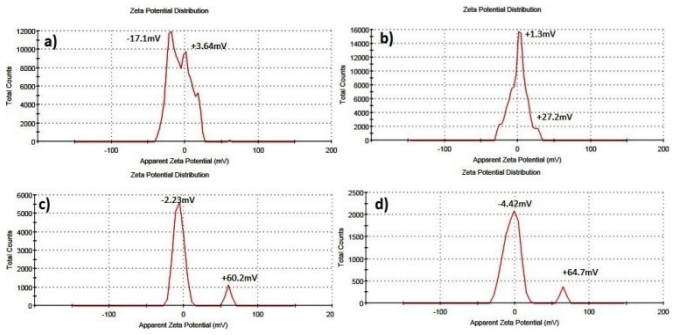

Fig. S5: Showing the surface potentials of (a) C1; (b) C2; (c) C1N; and (d) C2N.

Table S1: Showing the comparison of C1N and C2N (at λex 370nm and 420nm) in the terms of their LOD, *Ksv* and *Ka*.

	Property	C1N	C2N (λex 370nm)	C2N (λex 420nm)
LOD	Conc. Range (M)	$4.4x10^{-8}$ to $2.2x10^{-7}$	$4.4x10^{-8}$to $2.64x10^{-7}$	$8.8x10^{-8}$to $3.08x10^{-7}$
	R^2	0.954	0.9752	0.99602
	Slope	$1.557x10^{8}$	$8.027x10^{6}$	$7.013x10^{6}$
	SD	3.0308	0.13	0.0512
	LOD	**13ppb**	**11ppb**	**4.97ppb**
Ksv	Conc. Range (M)	$4.4x10^{-8}$ to $2.2x10^{-7}$	$4.4x10^{-8}$to $2.64x10^{-7}$	$4.4x10^{-8}$ to $2.2x10^{-7}$
	R^2	0.95175	0.96994	0.99428
	Ksv	**$2.02x10^{6}$ M^{-1}**	**$0.38x10^{6}$ M^{-1}**	**$0.48x10^{6}$ M^{-1}**
Ka	R^2	0.95486	0.88076	0.89764
	Ka	**$-3.8x10^{6}$ M^{-1}**	**$11.08 x 10^{6}$ M^{-1}**	**$21.5 x 10^{6}$ M^{-1}**

The FTIR study was conducted to confirm the EDA functionalization of C1, C2 QDs and their interactions with TNT (Fig. S6). In C1, the peak at 3395cm^{-1} is due to O-H stretching vibration while, the peaks at 1767cm^{-1} and 1327cm^{-1} are due to the C=O and C-O stretch of carboxylic groups present on C1 surface. After EDA functionalization of C1 to C1N, the decreased peak intensities at 1383cm^{-1} and 1432cm^{-1} denotes the involvement of carboxylic groups of C1 in bonding with amine group of EDA.[4]

In the spectrum of C1N (Fig. S6a), the broadening and increased intensity at 3100-3400cm^{-1}can be attributed to the N-H stretch of primary amines of EDA. The inefficient splitting of band at 3100-3400cm^{-1}may be due to the presence of secondary amines on C1N surface. The decreased in peak intensity at 1327cm^{-1} is due to C-N stretch which denotes the involvement of C-O of carboxylic groups in amide formation. The peaks at 1159$cm^{-1}$and 1638$cm^{-1}$are due to C-N stretch and N-H stretch respectively of amine groups which confirms the presence of EDA on C1 surface. In the spectra of C1N/T, the narrowing and decreased peak intensity of single band at 3395cm^{-1} can be attributed to the decreased primary amine N-H stretch that might be due to their involvement in JM complex formation with TNT. In C1N/T spectra, the again increase in peak intensities at 1575cm^{-1}, 1383cm^{-1} and 1482cm^{-1} are attribute to the N-

O stretch and C=C stretch of TNT aromatic ring respectively. The several bands at 950-1250cm^{-1}are due to the aromatic C-H in-plane bending vibrations.[5]

In C2 (Fig. S6b), the split band at 3100-3400cm^{-1}denotes the possible presence of nitrogen along with O-H stretching vibrations that might be due to the nitric acid treatment. The peaks at 1761cm^{-1}and 1382cm^{-1}denotes the oxy species vibrations i.e. C=O and C-O stretches of carboxylic groups. After EDA functionalization, the broadening and increase in intensity at 3000-3400cm^{-1} is resulted due to the N-H stretch of primary amine which further gets decreased in presence of TNT (C2N/T) due to their contribution in JM complex formation. The absence of C2N peak at 1761cm^{-1}shows the involvement of C-O in bonding with EDA. The peak at 1638cm^{-1}is due to C=O stretch of amides. The peaks at 1332cm^{-1}and 1157cm^{-1}are attributed to C-N stretch of primary and secondary amines respectively. In presence of TNT, the increased intensity at 1157cm^{-1}denotes the increase in secondary amines that might be involvement of C1N amine groups in JM complex formation. The increase in intensity at 1332cm^{-1}is due to the presence of N-O stretch in TNT nitro groups. The peak at 1432cm^{-1}and 1488cm^{-1}are attributed to the C=C stretch of TNT aromatic ring.[6]

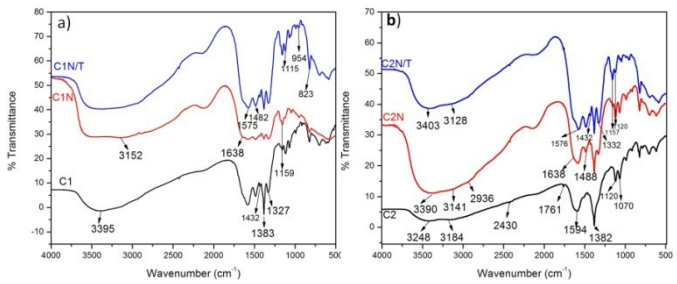

Fig. S6: Showing the vibrational characteristics of (a) C1, C1N, C1NT and (b) C2, C2N, C2NT.

The EDX data of C1N and C2N are shown in figure S7a and S7b respectively. In C1N, the atomic% of C, N and O are found to be 57.4%, 28.5% and 14.1% respectively. In C2N, the atomic% of C, N and O are found to be 37.72%, 33.94% and 28.29% respectively. While very little chlorine (0.05% at.) is also observed that might be due to some impurity during handling of sample and should be ignored.

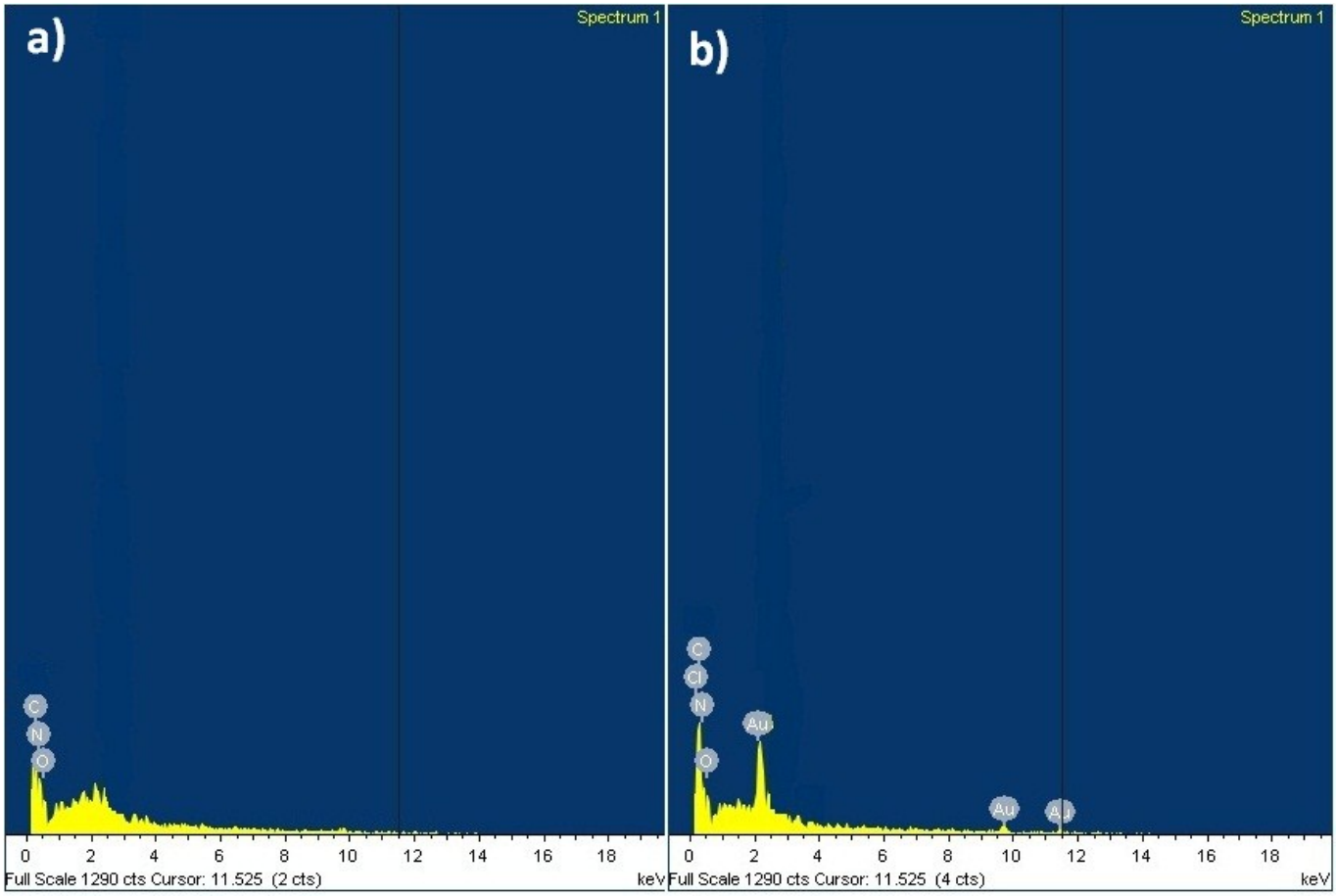

Fig. S7: Showing the EDX data of (a) C1N and (b) C2N.

The systematic execution of C1N and C2N concerning their selectivity towards TNT was also conducted against some of the very common interfering TNT analogues such as DNT, 2-TA, and NB (Fig.S8). It is observed that even at equal concentration of analogue compounds, TNT results in higher quenching in the emission intensity of C1N as well as C2N at λex 370nm and 420nm (Fig. S8a,c,e). The Q% of C1N in the presence of 1.76×10^{-7}M TNT, DNT, NB and 2-TA is 25.5%, 1.5%, 0.65% and 0.17% respectively (Fig. S8b). The Q% of C2N in the presence of 3.08×10^{-7}M TNT, DNT, NB and 2-TA at λex 370nm, is 31.8%, 13.7%, 11.1% and 9.9% respectively (Fig. S8d), while at λex 420nm is 26.8%, 16.1%, 10.9% and 9.1% respectively (Fig. S8f). It can be summarized that both the C1N and C2N in sure are highly selective for TNT although, some weak interactions may present between the amine moieties and these TNT analogue compounds. The possible mechanism behind the selectivity of these probes can be illustrated as; JM complex is a resonance stabilized sigma complex.[7] The three electron-withdrawing nitro groups enable the toluene ring of TNT to be electrophilic in nature which is enough for higher affinity of TNT to form the Meisenheimer complex with amine group. Due to which, JM complex formed by TNT is stabilized by

more resonance structures than the formed by other weaker Lewis acids like DNT, NB and 2-TA.[8,9] NB lacks the activating group at its ipso carbon.[10] The carboxylic group act as a deactivating group for SNAr in 2-TA.

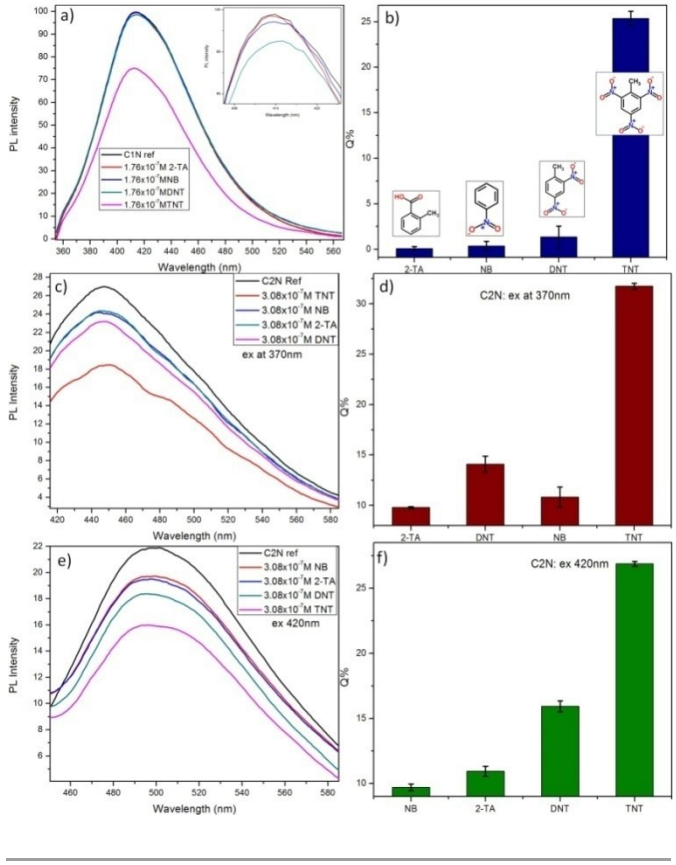

Fig. S8:(a), (c) and (e) Effect of TNT analogue compounds on the fluorescence intensity of C1N, C2N at λex 370nm and C2N at λex 420nm respectively; (b), (d) and (f) percentage quenching of C1N, C2N at λex 370nm and C2N at λex 420nm fluorescence respectively in the presence of various TNT analogue compounds with their chemical structures; [The magnified view of (a) is shown in its inset].

Owing to the high sensitivity and selectivity delivered by these CQDs probes (C1N and C2N), their feasibility was also vindicated against real tap water samples (CSIO) impaled with TNT. The TNT standard solution was added in tap water to achieve final 0.01, 0.1 and 1 ppm TNT concentration. The precision of these CQDs as a probe for TNT detection was decided by % recovery delivered [Table S2]. The results demonstrate that approximate analytical recoveries of the incorporated TNT in tap water samples ranged from 98% to 111% for C1N, 95% to 109% for C2N at λex=370nm and 98% to 102% for C2N at λex=420nm. This implicates that the sensing platform based on the amine functionalized CQDs as synthesized from vehicle soot, can efficaciously detect TNT in contaminated water samples to a

lowermost level of~5ppb level. In summary, the CQDs as synthesized from vehicle soot after the amine functionalization can additionally be scrutinized for explosive sensing applications.

Table S2: Showing the results for the determination of TNT in the real water samples using the developed materials.

Sample	Added (μM)	Found[a](μM) by C1N	%Recovery by C1N	Found[a](μM) by C2N		%Recovery by C2N	
				λex=370nm	λex=420nm	λex=370nm	λex=420nm
CSIO Tap water	0.0 (Control)	0.00	-	0.00	0.00	-	-
	0.044	0.0434± 0.028	98.7	0.0429±0.057	0.0436±0.06	97.63	99.23
	0.44	0.484±0.035	110.08	0.475±0.099	0.447±0.013	108.18	101.62
	4.4	4.649±0.04	105.66	4.2±0.022	4.35±0.0204	95.5	98.91

[a]Mean(n=3) ± standard deviation.

Moreover, these C1N delivered recommendable cell compatibility as shown in MTT assay results (Fig. S9A). MTT assay was performed to estimate the cell viability of different concentrations of C1N QDs and the same was compared with standard tissue culture plate without their addition as a control, whose cell viability was considered as 100%.[11] Mostly cells were observed to be viable at 2, 4, 6, 8, 10 and 20μg/mL of C1N. At 20μg/mL C1N, approximately 80.1% cells are viable as shown in figure S9A. So, the above study shows that mostly cells are viable at all C1N concentrations.

Relying on their biocompatibility, the potential of C1N in the detection of TNT in cells was ascertained by fluorescence-based imaging (Fig. S9B). Accordingly, the C1N emission signal emerging from the TNT incubated cells was evaluated. When the cells were treated with C1N alone, strong blue and green emission was observed in the cytoplasm of the cells (Fig. S9e, f).[12] This dual emission behavior observed is in accordance with the excitation dependent emission behavior of these C1N (discussed in Fig. 6b). Contrarily, when TNT pre-treated cells were exposed to C1N, a marked decrease in blue as well as green fluorescence emissions of the cells was apparent due to intracellular interactions with TNT (Fig. S9h, i). Therefore, changes in the fluorescence emission intensity of C1N could be used as an indicator for the detection of TNT affected cells.

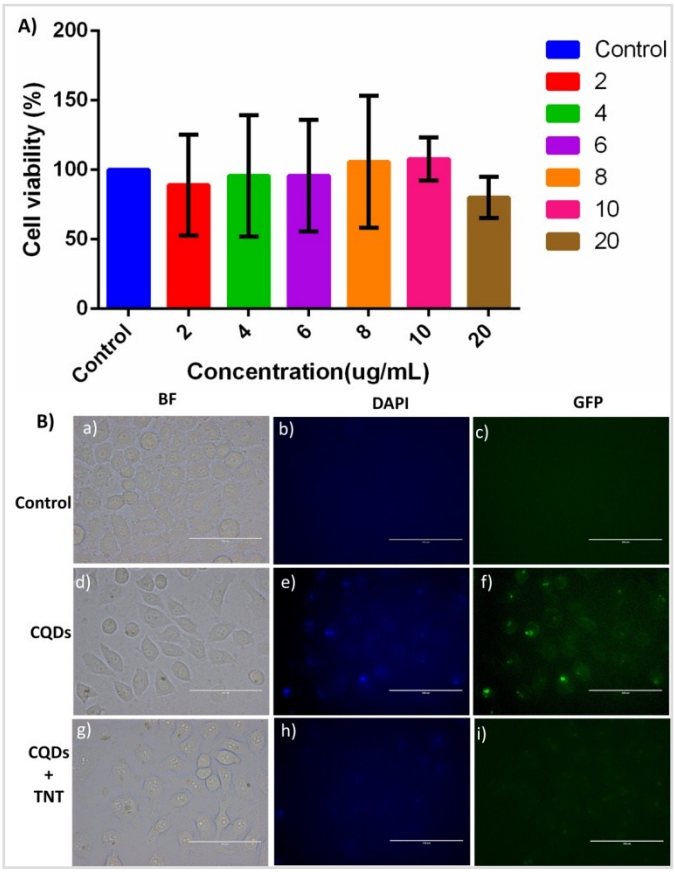

Fig.S9: A) In vitro cell viability of L-132 cells treated with various concentrations of C1N as estimated by the MTT assay; B) Fluorescence microscopy images of only L-132 cells as control (a-c); L-132 cells treated with of C1N only (d-f) and L-132 cells pre-treated with 4ppm TNT followed by the addition of equivalent C1N (g-i). The scale bar for the images is 100 µm. Filters: DAPI (λex = 360 nm, λem = 447 nm); GFP (λex = 470 nm; λex= 525 nm).

References

1 S. Paikaray, *PhD diss.*, 2013, pp 8-9.
2 Kleinauskas, S. Rocha, S. Sahu, Y.-P. Sunand P. Juzenas, *Nanotechnology*, 2013, **24**, 325103.
3 Q. Wang, C. Zhang, G. Shen, H. Liu, H. Fuand D. Cui, J. Nanobiotechnol, 2014, **12**, 58.
4 J. Coates, *Encyclopedia of Anal. Chem.*, 2000, 10815–10837.
5 S. Devi, B. Singh, A. Paul and S. Tyagi, *Anal. Methods*, 2016, **8**, 4398-4405.
6 R. Silverstein, G. Bassler and T. Morrill, *Spectrometric Identification of Organic Compounds*, 4th ed. John Wiley & Son: New York, 1998.
7 W. Danikiewicz, T. Bieńkowski, D. Kozłowska and M. Zimnicka, *Journal of the American Society for Mass Spectrometry*, 2007, **18**, 1351-1363.
8 J. Li, C. E. Kendig and E. E. Nesterov, *Journal of the American Chemical Society*, 2007, **129**, 15911-15918.
9 J. Clayden, N. Greeves and S. Warren, Oxford University Press, 2001.
10 M. K. Stern and B. K. Cheng, *The Journal of Organic Chemistry*, 1993, **58**, 6883-6888.
11 A. Sachdev and P. Gopinath, *Analyst*, 2015, **140,** 4260 –4269.
12 A. Sachdev, I. Matai and P. Gopinath, *RSC Adv.*, 2014, **4**, 20915–20921.